CrossMark

ORIGINAL PAPER

Determining the Particle Size of Debris from a Tunnel Boring Machine Through Photographic Analysis and Comparison Between Excavation Performance and Rock Mass Properties

A. Rispoli[1] · A. M. Ferrero[1] · M. Cardu[2] ⓘ · A. Farinetti[3]

Abstract This paper presents the results of a study carried out on a 6.3-m-diameter exploratory tunnel excavated in hard rock by an open tunnel boring machine (TBM). The study provides a methodology, based on photographic analysis, for the evaluation of the particle size distribution of debris produced by the TBM. A number of tests were carried out on the debris collected during the TBM advancement. In order to produce a parameter indicative of the particle size of the debris, the coarseness index (CI) was defined and compared with some parameters representative of the TBM performance [i.e. the excavation specific energy (SE) and field penetration index (FPI)] and rock mass features, such as RMR, GSI, uniaxial compression strength and joint spacing. The results obtained showed a clear trend between the CI and some TBM performance parameters, such as SE and FPI. On the contrary, due to the rock mass fracturing, a clear relationship between the CI and rock mass characteristics was not found.

Keywords Debris size distribution · Photographic analysis · Field specific energy · Coarseness index · TBM performance · Hard rock TBM

✉ M. Cardu
  marilena.cardu@polito.it

1 Department of Earth Sciences, Università degli Studi di Torino, Turin, Italy

2 DIATI-Politecnico di Torino; IGAG-CNR, Turin, Italy

3 Tunnel Euralpin Lyon Turin (TELT) sas, Turin, Italy

1 Introduction

Excavation by tunnel boring machines (TBMs) in hard rock-like environments is the most commonly adopted technique in tunnel projects longer than 1 km because of the considerable advantages gained in terms of time and development costs. The successful use of this technique relies on the proper design of the cutterhead, which is strongly dependent on the characteristics of the material under excavation. TBM performance is thus conditioned by finding, during excavation, conditions similar to those provided at the design stage. For these reasons, in order to evaluate the efficiency of the excavation, the definition of the actual conditions of the rock mass cannot be disregarded in the performance evaluation. In this regard, the particle size of the debris produced during excavation is able to provide information on both cutting efficiency and characteristics of the rock mass.

Numerous studies have examined the relationship between the size of the debris particles and some of the machine's performance indicators (e.g. Roxborough and Rispin 1973; McFeat-Smith and Fowell 1977; Altindag 2003; Tuncdemir et al. 2008; Balci 2009; Abu Bakar et al. 2014). In particular, the specific energy (SE), which is an indicator of the efficiency of the excavation and defined as the energy needed to excavate a unit volume of rock, assumes, for a given rock and type of tool, a decreasing trend with increasing particle size obtained from the rock fragmentation process. This condition is easily detectable in the laboratory (Roxborough and Rispin 1973) but also on site, as evidenced by the results obtained by Tuncdemir et al. (2008). Farrokh and Rostami (2008) and Balci (2009) also found that the presence of discontinuities and other structural features in the rock influence the debris size.

2 Springer

The systematic on-site assessment of the particle size obtained in a TBM excavation, however, is not simple and the particle size distribution of the debris is normally very wide. The theory of rock-breaking mechanics, with regard to disc tools, involves the detachment of rock chips along with pulverised and granular rock. Gertsch et al. (2000) noticed that the size of the chips depends on the spacing of the disc tools, as well as on the penetration value taken during each revolution of the cutterhead. However, under fractured rock mass conditions, the particle sizes of the debris can be significantly larger because of the displacement of rock blocks due to the presence of crossing joints (Farrokh and Rostami 2008). For these reasons, the particle size distribution of the debris may include both pulverised rock and fragments with dimensions up to several tens of centimetres.

Under such conditions, several problems would complicate use of the traditional classification method of sieving (coarse part) and sedimentation (fine part). First, it would be necessary to manually measure each fragment by means of a series of screens because sieves are unsuitable for the analysis of blocks of decimetric dimensions. Moreover, as the weight of the representative volume required to analyse each sampling is dependent on the maximum size of the fragments, its result would be considerably high [i.e. at least 40 kg for a maximum size of 63 mm (British Standard European Norm 933-1 2012)] and thus a comprehensive analysis would be highly time-consuming. Finally, in order for the debris collected for the sieving test to be representative, it should be taken directly from the conveyor belt, as suggested by Bruland (1998). As a consequence, this condition would affect the excavation cycle, as it is not recommended to stop the belt before downloading.

In order to address the problems above, the present study proposes a methodology for the analysis of debris from TBM through photographic analysis. This method, previously adopted by Rispoli et al. (2016), allows quick analysis of a large volume of debris (about 3 m^3 for each sampling) with controlled costs. Additionally, it does not require laboratory analysis or extensive labour (e.g. both the sampling and the processing phases may be carried out by one operator). Due to its simplicity, the method is systematically implementable on a daily basis, together with other investigations carried out during the advance of the TBM, and does not interfere with the excavation cycle because the sample is taken from the piles of debris outside the tunnel.

The proposed method is based on the determination of a 3-D volume of debris through the processing of images appropriately taken from isolated portions of the piles. For this purpose, the Split Desktop 3.1 software, distributed by Split Engineering LLC (www.spliteng.com), is employed. The coarse fraction is determined via direct assessment of the fragments observed in the image, whereas the finer part is the result of a statistical estimation. For this reason, it is often chosen to detail only the coarse part of the analysed samples (e.g. size greater than about 10 mm). In this regard, Farrokh and Rostami (2008) correlated the tunnel convergence with the size distribution of the debris estimated by visual observation of rock fragments in the muck cars. They did not analyse the particle size distribution of fragments smaller than 2 cm and claimed that the portion of debris with sizes between 2 and 10 cm represented the ground conditions where the face is stable and actually being excavated.

The results presented in this study are based on a campaign analysis carried out in the Maddalena exploratory tunnel, excavated with a 6.3-m-diameter TBM while crossing the Clarea complex, which is mainly characterised by mica-schists and with rock mass rating (RMR) between 41 and 80. The results related to the particle size distribution of the debris are compared with some parameters representative of the TBM performance [i.e. the excavation SE and the field penetration index (FPI)] and with the rock mass features [RMR, geological strength index (GSI), uniaxial compression strength (UCS) and joint spacing]. In particular, in order to provide a parameter indicative of the particle size of the debris, the coarseness index (CI) is properly revised with respect to that originally proposed by Roxborough and Rispin (1973) and employed in several other studies (e.g. McFeat-Smith and Fowell 1977; Altindag 2003; Tuncdemir et al. 2008; Balci 2009; Abu Bakar et al. 2014).

2 Study Site

2.1 General Information

The site under investigation is the Maddalena exploratory tunnel. This is one of four preliminary works in the construction of the new Turin–Lyon link, which will extend for 57 km between Susa (Piedmont, Italy) and Saint-Jean-de-Maurienne (Savoy, France). The Maddalena exploratory tunnel, originally designed with a length of 7.5 km, was completed with a final length of approximately 7 km. The tunnel has a diameter of 6.3 m and was excavated by means of an open TBM, excluding the first 200 m.

This approach was adopted because of the geognostic purpose of the tunnel and its applicability due to the good conditions of the rock mass. This tunnel serves to deepen the knowledge on the geological and geomechanical characteristics of the rock mass and verify the performance of the adopted excavation technique. Additionally, it will be used as a service tunnel when the new Turin–Lyon link becomes operational.

2.2 Geological Conditions

Two main metamorphic formations were encountered along the tunnel path: the Ambin and the Clarea complexes. The geological setting is shown in Fig. 1. After the first 200 m, characterised by Quaternary deposits and Piedmont Zone units (calcschists, marbles and cargneules along a main detachment zones), the tunnel crossed the Ambin complex (AMC), which is dominantly composed of aplitic gneiss and extends for approximately 1 km. The contact zone (AMD) was encountered, which extends for a few hundred metres between the two main units and is composed of alternations of quartz mica-schist and gneiss (albite). The remaining 6 km cross the Clarea complex (CLR), which is substantially characterised by Clarea mica-schist. Results presented in this study refer to samples taken within the CLR, which has an RMR ranging from 41 to 80. The tunnel crossed areas with low average permeability, which developed when passing through sub-vertical fault zones.

2.3 TBM Characteristics

The machine employed was a single-gripper open-HP Robbins TBM with a diameter of 6.3 m and an overall length of 240 m. The main technical characteristics are summarised in Table 1. Muck haulage was accomplished by means of a conveyor belt, which discharged the cuttings outside the tunnel in a portion of the yard used as a storage area.

Table 1 Technical characteristics of the TBM

Cutterhead thrust—recommended	12,800 kN
Maximum machine thrust	13,700 kN
Cutterhead power	2202.8 kW
Cutterhead torque	2082.9 kN m
Cutterhead speed	0–10.8 rpm
Number of main thrust cylinder	4
Thrust cylinder stroke	1800 mm
Hydraulic system power	111.9 kW
Gripper total force	36,400 kN
Numbers of disc cutters	43
Disc cutters size	17″ (431.8 mm)

2.4 TBM Data

The recording of the TBM data was performed using an automatic detection and data logging system that can read, view and collect the most significant excavation parameters, such as cutterhead torque, total thrust, cutterhead rotational speed, rate of penetration, gripper pressure, thrust cylinder advance, TBM excavation state and tunnel chainage. The collected data were available in real time through a server.

In order to optimise the study of TBM performance, a set of Matlab scripts was specially developed for the machine data management. These codes allow one to:

- create a database that collects both the machine and related geomechanical data of the examined rock mass;
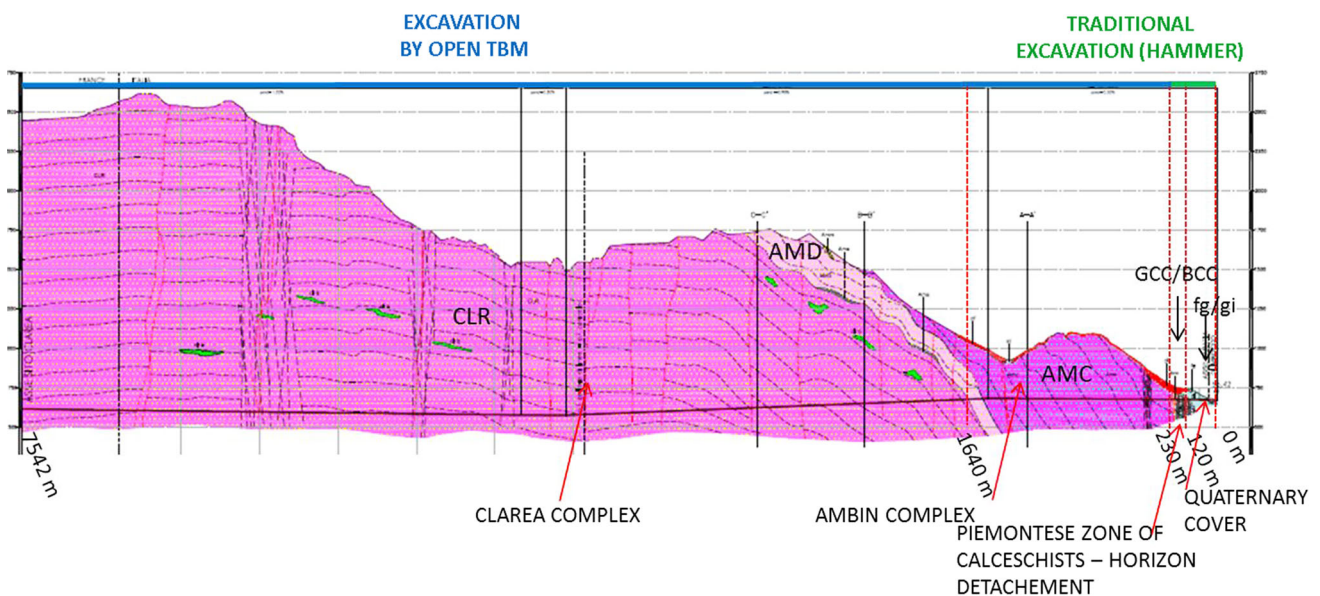

Fig. 1 Geological context of the Maddalena exploratory tunnel (Parisi et al. 2015)

- determine some machine parameters characteristic of the excavation efficiency derived from those recorded by the TBM (e.g. Balci 2009; Hassanpour et al. 2011; Bilgin et al. 2014);
- filter the data as a function of the study to be carried out;
- consult the data in an optimal way.

The derived parameters of the TBM presented in this study were obtained using the following equations:

$$F_{\mathrm{N}} = \frac{\mathrm{FT}}{N_{\mathrm{cutter}}} \quad \mathrm{FPI} = \frac{F_{\mathrm{N}}}{\mathrm{ROP}} \quad \mathrm{SE} = \frac{2 \cdot \pi \cdot \mathrm{RPM} \cdot T}{\mathrm{PR}} \quad (1)$$

where F_{N}: mean cutter load or normal force (kN/cutter); FT: total thrust exerted by the cutterhead (kN); N_{cutter}: number of cutters; FPI: field penetration index (kN/cutter/mm/rev); ROP: rate of penetration (mm/rev); SE: field specific energy (MJ/m^3); RPM: rotational speed (rev/min); T: cutterhead torque (MN m); PR: penetration rate (m^3/min).

It should be noted that the total thrust registered during the excavation also includes friction losses.

2.5 Rock Mass Data

The investigation and monitoring of rock mass during the tunnel excavation included extensive tests both on site and in the laboratory. This study refers to the results obtained by geological/geomechanical surveys carried out on a daily basis (about every 10 m of excavation) on the tunnel walls, in accordance with suggestions by the International Society for Rock Mechanics (1978). In particular, the following rock mass parameters were analysed: RMR (Bieniawski 1989); GSI (Hoek et al. 1998); joint spacing and UCS, obtained via the point load test following the suggestions of Broch and Franklin (1972). It should be noted that the UCS determined during the crossing of the Clarea mica-schists corresponds to the average between values obtained perpendicular and parallel to the schistosity.

3 Methodology

3.1 Split Desktop Software

Split Desktop is an image processing software primarily used in the mining and mineral industry to estimate the size distribution of rock fragments in the various production stages. Using one or more photographic images of rock fragments, it is possible to determine the 3-D volumes of fragments via image processing and appropriate statistical calculations (Kemeny 1994). In particular, the software outlines the rock fragments contained in the image in order to determine the contours and consequently the 2-D dimensions through an almost entirely automated process. From these results, the 3-D sizes of the fragments are evaluated by means of suitable algorithms, which, compared with those of a series of virtual sieves defined by the user, allow for the determination of the particle size distribution of the rock fragments.

It is noteworthy that a dimension called "cut-off" is defined during the processing phase, below which the software is no longer able to recognise the fragments of rock, as they are too small compared to the image resolution. The particle size distribution of the material recognised with dimensions greater than the cut-off is determined by the direct processing of the surfaces outlined in the image. As for the portions whose dimensions are lower than the cut-off, the software refers to specific statistical distribution relations attributed to the finer material.

3.2 Sampling

Approximately 3 m^3 of debris discharged from the conveyor belt was picked up from one of the storage heaps outside the tunnel by means of a wheel loader. It is important to sample from the newly deposited material in order to track the time of excavation and relative chainage of the tunnel. The sample taken was then moved to an adjacent location where it could be analysed without interfering with other activities of the heading. The material was spread so as to create a flattened surface in order to optimise the photographic analysis results by reducing the geometric distortion. At this point, nine photographs were taken of the portion of debris using a high-resolution camera according to the following steps (Fig. 2):

- One photograph of the muck pile was taken to obtain an overall picture;
- The muck pile was virtually divided into four parts;
- For each part, two photographs were taken: one closer (horizontal length of the image of about 50 cm) and the other at a larger distance (horizontal length of 1–1.5 m) in order to cover different scales, which allows reliable analysis of a broader range of fragments sizes;
- Before taking each photograph, two objects of known size were placed on the pile as a scale. In this study, two 6-cm-diameter rubber balls were used.

At this point, the material was relocated in the original muck pile and the sampling phase was complete. This step was performed in about 10 min.

3.3 Image Processing

In order to achieve a good compromise between representativeness of the sample and analysis times, the
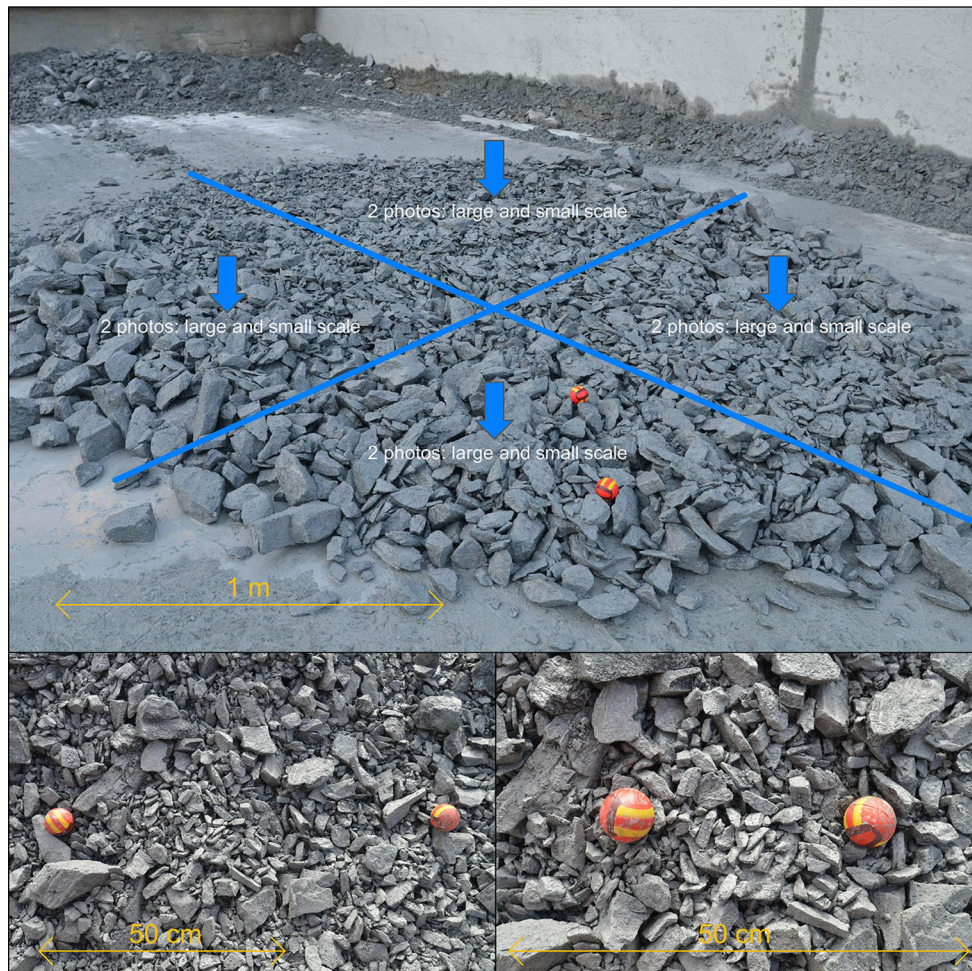
Fig. 2 Above: Subdivision of the muck pile into four parts with two photographs taken at different scales for each. Below: Photographs of the same portion of the muck pile taken at large scale (*left*) and small scale (*right*)

processing phase affected only two of the four parts into which the sample was divided. Reference was made to two opposite portions according to the principle of quartering (Gertsch et al. 2000). For each sample, four pictures were then processed, considering that two photographs for each portion of the sample were taken, both large and small scale. Each photograph was processed in the following steps:

- Image loading using the software;
- Automatic delineation of individual rock fragments in the image;
- Definition of the scale using the reference objects in the image;
- Manual modification of the automatic delineation. This is necessary if significant inaccuracies were found in the phase of delineation of the fragments performed by the software. However, it is a good rule to always perform a manual edit in order to optimise the processing result;

- Definition of the "fines factor"; namely, the amount of fines present in the portions of the image that the software is unable to sketch. In the current study, the "fines factor" was chosen to be equal to 10% of the volume by applying the recommended guidelines from the software developers. Reference was made to the characteristics of the debris found on average and the value was kept constant for all analysed images so as to successfully perform the comparison between different samples from the same site.

The overall duration of the processing phase varied substantially according to the duration of the manual-editing phase, which depends on user discretion according to the desired degree of precision. In the present study, an optimal processing level was obtained by allocating approximately 20–30 min for each image.

At this point, the software was able to obtain the grain size analysis results, both graphically and analytically. A particularly advantageous aspect of the photographic

approach, compared to that of sieving, is the result customisation. It is possible to choose the size of the virtual sieves used in the evaluation of the particle size according to the aims of the study. Some of the main processing stages performed by Split Desktop are depicted in Fig. 3.

As previously mentioned, for fragments of sizes greater than the cut-off, Split Desktop performs a direct evaluation based on the graphic processing of the image. As for the finer fragments, the results are obtained by means of a statistical estimation. Accordingly, in order to refer only to the results derived from the direct evaluation of the software, it was decided in this study to refer to the portion of the grain size distribution above the cut-off (about 10 mm for the performed analysis).

3.4 Calculation of the CI

The CI is a dimensionless number that provides a comparative measure of the size and distribution of the produced debris (McFeat-Smith and Fowell 1977). Roxborough and Rispin (1973) originally calculated the CI as the sum of the cumulative weight percentages retained on each sieve used. In this study, the CI was calculated as shown in Table 2. While the original cumulative percentage approach refers to the volume of the fragments obtained from the analytical results provided by Split Desktop, the reference size of sieves were revised in the present study in accordance with the choice to study only the coarse portion of the sampled debris.
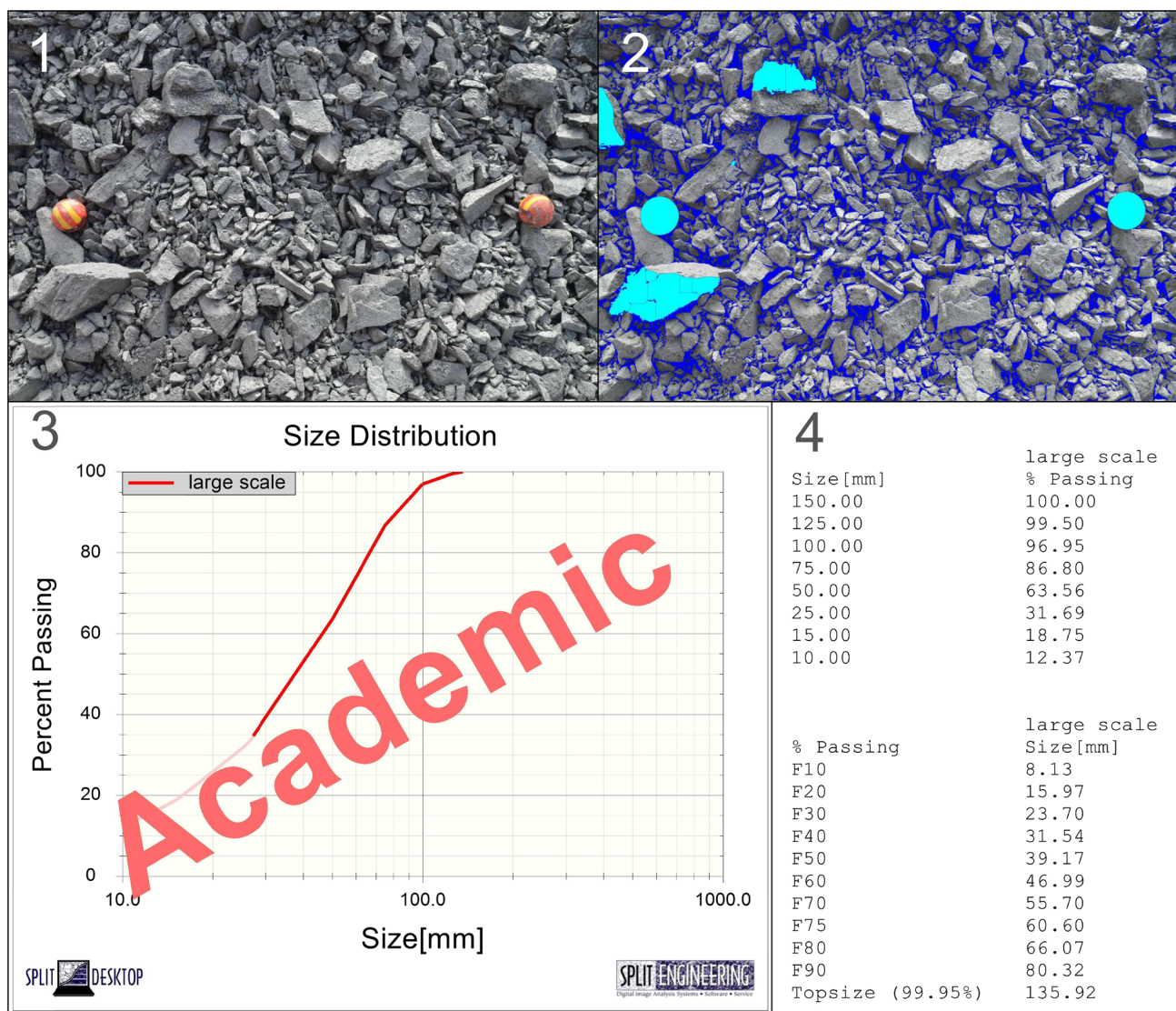

Fig. 3 Some processing steps using the Split Desktop software: (1) loaded image; (2) outlined and scaled image; (3) graphical restitution of the result; and (4) analytical restitution of the result (Cardu et al. 2017)

Table 2 Example of coarseness index (CI) calculation

Size fraction (mm)	Retained (%)	Cumulative retained (%)
+100	1.4	1.4
−100 + 75	3.5	4.9
−75 + 25	46.8	51.7
−25 + 10	25.6	77.3
−10	22.7	100.0
Total	100.00	CI = 235.2

3.5 Data Processing

In order to compare results obtained by photographic analysis with those obtained by other investigations, it is necessary to classify the debris as a function of the chainage where it was produced. The definition of the chainage is related to the determination of the time displayed by the TBM based on the following relationship:

$$TBM_{time} = Image_{time} \pm \Delta time_{TBM-Image} - Belt_{time} - Loader_{time} \qquad (2)$$

where TBM_{time} is the time shown by the TBM clock used to assess the machine data; $Image_{time}$ is the time when the first picture of the tested muck pile was taken (i.e., time displayed by the camera); $\Delta time_{TBM-Image}$ is the discrepancy between the clock of the TBM and that of the camera; $Belt_{time}$ is the time taken for the debris to be transported on the conveyor belt from the excavation face to the outside muck pile according to the chainage reached and the speed of the conveyor belt; $Loader_{time}$ is the time required by the wheel loader to load and arrange the material.

Once the TBM_{time} is defined, it is possible to go back to the machine data over a range of ± 10 min in order to optimally assess the variability of parameters and to take note of any discrepancies with the estimations made (e.g. stops, slopes, jumps of the conveyor belt). An example is shown in Fig. 4.

4 Results

Table 3 lists the results obtained from nine debris samples taken while crossing the CLR (Fig. 1). Specifically, the results of the particle size distribution are included together with the related TBM data and rock mass parameters.

The results from the debris also include three parameters that express the average characteristics of the coarse portion of the debris: the D_{50}, also known as the median diameter or the medium value of the particle size distribution, which expresses the value of the particle diameter at 50% in the cumulative distribution; the D_{max}, which the

software defines as 99.95% in the cumulative distribution; and the ratio, D_{75}/D_{50}, which is indicative of the degree of uniformity of particle size distribution. High values of D_{50}, as well as high CI values, correspond to a larger average particle size and, consequently, lower fragmentation.

As specified above, data on the rock mass characteristics refer to the results of geomechanical surveys carried out in the tunnel section from which the analysed debris was taken. It is also shown that the values of the pairs A–B, C–D and E–F belong to samples taken on the same day along intervals of several hours. For this reason, the mentioned pairs of samples show the same values of rock mass parameters, given the daily basis of the geomechanical survey.

4.1 Grain Size Distribution

The particle size distribution of the coarse portion of the analysed samples is shown in Fig. 5. It shows how the samples E and F differ considerably from the other tested samples in their demonstration of a significantly finer particle size detectable in the CI values, as well as in the noticeably smaller values of D_{50} and D_{max}. All samples show a fairly wide size distribution in the range 10–200 mm. This can be highlighted, in addition to the trends of particle size distribution, by the values of D_{75}/D_{50} ratio, for which all fall within 1.6 and 2. This condition shows that there is no relationship between this ratio and the analysed parameters for the samples examined.

4.2 TBM Parameters Versus Grain Size Distribution of the Debris

In this section, the trends of the machine parameters are discussed, which express the performance of the TBM, depending on the CI. Among these, there is noticeable correlation between the SE, which is indicative of the excavation efficiency, and CI (Fig. 6). It is known from mechanical rock-boring theory that, for a given rock, larger size particles involve lower SE consumption (Ozdemir 1992). Figure 6 shows how the inverse trend between SE and CI, which has been highlighted in several previous studies (e.g. Roxborough and Rispin 1973; Tuncdemir et al. 2008; Abu Bakar et al. 2014), is also noticed in the experimental results obtained in this research.

Figure 7 shows the values of the FPI as a function of the CI. The downward trend of FPI when CI increases is notable. Keeping in mind that low values of FPI correspond to a greater susceptibility of the rock mass to be penetrated, lower fragmentation is obtained where rock portions are more easily penetrable on the examined site.

Figure 8 shows a reverse trend between F_N and CI, which implies that the particle size decreases when the

Fig. 4 Example of evaluation of the cutter normal force (F_N) and rate of penetration (ROP) with TBM$_{time}$ estimated at around 11:56 h. The time covers a range of ± 10 min
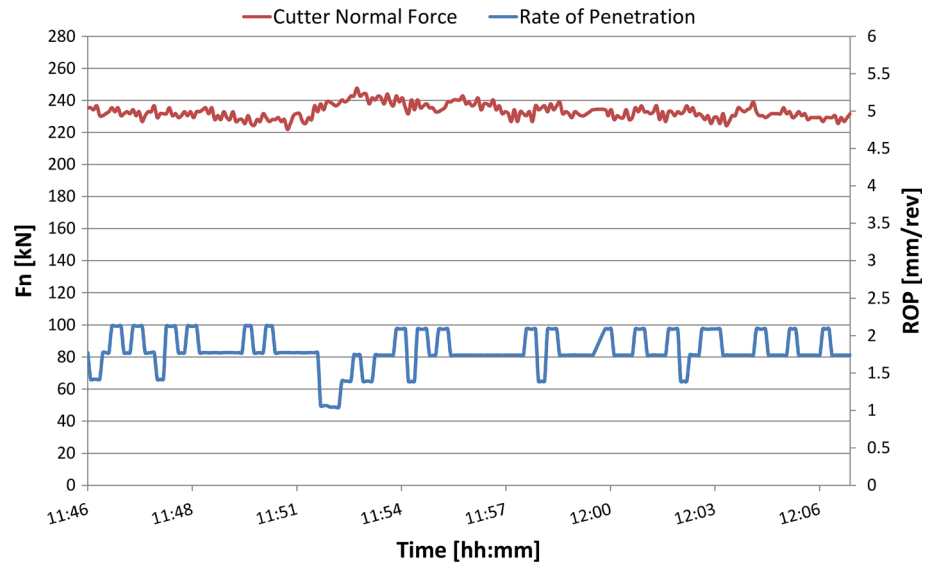
thrust applied to the cutterhead increases. This is in contrast to what usually takes place (Ozdemir 1992; Tuncdemir et al. 2008), where an increase in the thrust force applied to the disc tools implies an increase in the penetration, which results in a larger average size of the rock chips produced. The relationship between the CI and rate of penetration (ROP), shown by Roxborough and Rispin (1973) in the intact rock, is not observed in the examined case. In fact, in the rock type tested, it is shown in Fig. 9 that the CI shows a series of quite dispersed values with respect to ROP. These conditions are mainly attributable to the fracturing of the rock mass. Several studies show that both the rate of penetration and the particle size distribution of the debris are strongly influenced by the rock mass characteristics and especially by its fracturing. Previous studies that either analysed field data (Nelson 1993) or employed 2D numerical models (Gong et al. 2006) reported that the joint spacing affects the FPI and the ROP. Balci (2009) pointed out that, in contrast to the theory and laboratory tests on intact rock (e.g. Roxborough and Phillips 1975), the thrust applied to the cutterhead and the ROP do not show any relationship. This condition, which can also be found in the F_N and ROP values obtained at the present study site (Fig. 10), can be attributed to the effect of frictional forces induced on the cutterhead by the collapse of some rock mass portions at the crown and face of the tunnel.

Abu Bakar et al. (2014) have shown that both the production rate and chip size achieved in the field can differ significantly from results obtained in the laboratory. In particular, the presence of fractures within the rock mass seems to have different effects on the CI. On the one hand, fracturing of the rock mass may induce a decrease in the CI, compared to the intact rock conditions, due to the

greater presence of fines caused by over-crushing in front of the cutterhead (Balci 2009). On the contrary, fracturing at the excavation face can cause breakage and the release of rock blocks bigger than those provided by the standard process of chip formation (Farrokh and Rostami 2008).

Finally, Fig. 11 shows that no significant trend is observable between the torque and the CI.

4.3 Grain Size Distribution of Debris Versus Rock Mass Parameters

Figure 12 shows that there is no noticeable relationship between the CI and RMR. This condition, which can also be observed between the CI and GSI (Fig. 13), shows how the applied geomechanical classifications may be unable to establish a clear relationship with the degree of rock breakage in TBM operations. Figure 14 illustrates the downward trend of the CI as UCS increases. Referring to the values given in Table 3, it can be stated that the particle size does not show a clear relationship with the joint spacing in the examined sections of the tunnel. This result seems to confirm what was previously discussed, namely that the CI may not show a statistical relationship to the joint spacing.

5 Conclusions

Particle size distribution of debris produced by excavation using a TBM, as well as determining the possible reuse of the material (Gertsch et al. 2000), can provide important information on both the performance of the excavation machines (Roxborough and Rispin 1973; Tuncdemir et al. 2008) and the rock mass characteristics (Balci 2009; Abu

Table 3 Particle size analysis results and parameters related to the TBM and the rock mass of nine samples taken while crossing the Clarea Complex in Maddalena exploratory tunnel

Sample reference			A	B	C	D	E	F	G	H	I
Sieve size (mm)	200	Passing (%)	100.0	100.0	100.0	100.0	100.0	100.0	100.0	100.0	100.0
	150		100.0	100.0	99.8	96.0	100.0	100.0	96.9	98.0	98.8
	125		99.9	100.0	98.5	92.1	100.0	100.0	93.6	92.8	94.9
	100		98.6	98.8	94.2	86.0	100.0	100.0	87.8	81.9	88.1
	75		95.1	92.6	84.3	74.7	99.6	99.2	76.7	66.7	76.5
	50		82.7	73.4	66.7	56.6	94.3	94.2	57.8	50.1	59.9
	25		48.3	44.1	39.8	33.4	73.6	71.3	29.4	34.0	39.4
	15		31.9	30.2	27.2	22.7	55.0	50.8	17.4	25.7	30.3
	10		22.7	22.4	20.2	16.7	42.4	38.2	11.5	20.3	24.2
Size fraction (mm)	+ 100	Cumulative retained (%)	1.4	1.2	5.8	14.0	0.0	0.0	12.2	18.1	11.9
	−100 + 75		4.9	7.4	15.7	25.3	0.4	0.8	23.3	33.3	23.5
	−75 + 25		51.7	55.9	60.2	66.6	26.5	28.7	70.6	66.0	60.6
	−25 + 10		77.3	77.6	79.8	83.3	57.6	61.8	88.5	79.8	75.8
	−10		100.0	100.0	100.0	100.0	100.0	100.0	100.0	100.0	100.0
Muck parameters		CI	235.2	242.1	261.5	289.2	184.5	191.2	294.6	297.1	271.8
		D_{50} (mm)	26.0	29.6	33.5	42.4	12.9	14.7	42.1	49.9	37.3
		D_{75}/D_{50}	1.6	1.7	1.8	1.8	2.0	1.9	1.7	1.8	1.9
		D_{max} (mm)	126.8	114.2	164.1	189.3	80.1	95.6	196.5	175.7	165.6
TBM data		F_N (kN)	243.7	217.2	193.1	130.9	232.7	205.1	112.6	92.7	77.0
		±	7.8	16.9	16.6	14.7	4.5	26.8	6.0	15.6	11.8
		RPM (rev/min)	8.2	7.8	7.6	6.9	9.5	8.8	5.1	8.4	4.3
		±	0.0	0.4	0.3	0.5	0.1	0.7	0.0	0.3	0.2
		ROP (mm/rev)	2.2	3.6	4.4	3.9	1.8	2.5	3.6	1.9	2.3
		±	0.4	0.8	0.7	0.8	0.2	0.7	0.5	0.6	1.0
		FPI (kN/cutter/mm/rev)	108.7	60.2	43.6	33.9	129.0	82.8	30.9	48.3	33.5
		±	23.5	17.8	10.3	11.1	19.8	34.8	6.0	23.9	19.7
		Toque (kN m)	579.8	738.9	748.4	531.5	453.0	529.6	297.0	197.2	229.2
		±	77.4	157.9	128.9	138.9	48.9	147.7	62.8	77.3	212.5
		SE (MJ/m^3)	52.2	41.0	34.0	27.5	50.6	43.3	16.4	20.7	20.0
Rock mass characteristics		Lithology	Mica-schist	Mica-schist	Mica-schist	Mica-schist	Mica-schist	Mica-schist	Mica-schist	Mica-schist	Mica-schist
		RMR	61	61	71	71	63	63	54	53	56
		GSI	65	65	75	75	63	63	60	57	60
		Joint spacing (cm)	50–100	50–100	100–200	100–200	20–50	20–50	20–50	50–100	50–100
		UCS (MPa)	174	174	164	164	181	181	144	165	153

TBM data: F_N cutter normal force, *RPM* rotational speed of the cutterhead, *ROP* rate of penetration, *FPI* field penetration index, *Torque* cutterhead torque, *SE* field specific energy

Bakar et al. 2014). However, the on-site determination of the particle size by systematic sieving is not easy to implement in terms of time and cost. The study presented here provides a methodology based on photographic analysis, which allows for the determination of size distribution of the coarse portion of the debris produced in a fast and economical way without interfering with the excavation cycle. The results obtained from the analysis of nine samples of debris collected during the crossing of a lithological unit, predominantly consisting of mica-schists,

were compared to the TBM performance and rock mass characteristics.

The results obtained show how the CI follows a reverse trend with respect to the SE, in agreement with theory and various investigations both in laboratories and on-site. The comparison between the FPI and CI shows that, as the susceptibility of the rock mass to penetration increases, there is also an increase in the size of the fragments. It is shown that an increase in the force applied to the cutterhead leads to an increase in the fragmentation of the
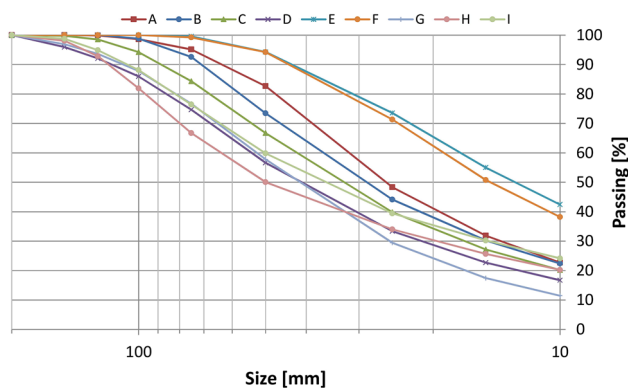
Fig. 5 Grain size distribution of the nine analysed samples
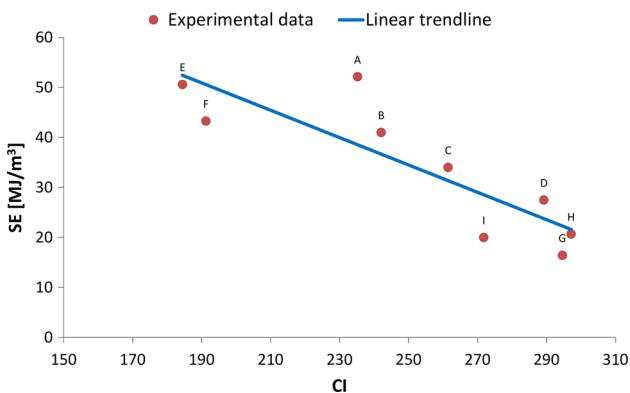

Fig. 6 Field specific energy (SE) versus coarseness index (CI). Linear trendline: $SE = -0.2737 \cdot CI + 102.91$; $R^2 = 0.734$
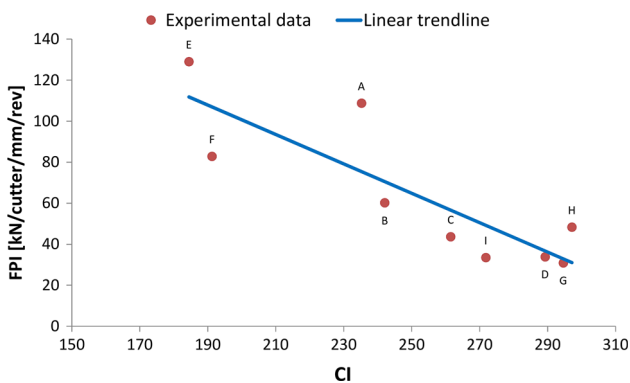

Fig. 7 Field penetration index (FPI) versus coarseness index (CI). Linear trendline: $FPI = -0.7168 \cdot CI + 244$; $R^2 = 0.723$
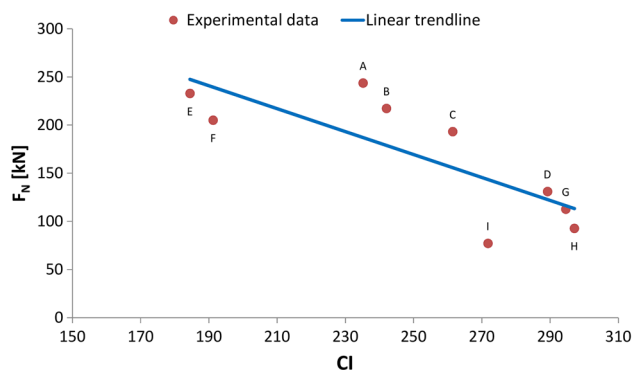

Fig. 8 Cutter normal force (F_N) versus coarseness index (CI). Linear trendline: $F_N = -1.1909 \cdot CI + 467.19$; $R^2 = 0.622$
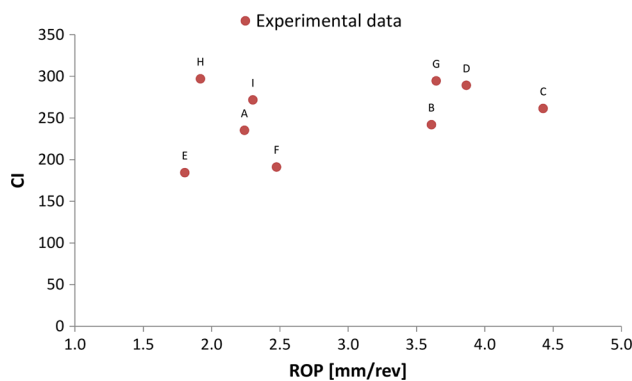

Fig. 9 Coarseness index (CI) versus rate of penetration (ROP)
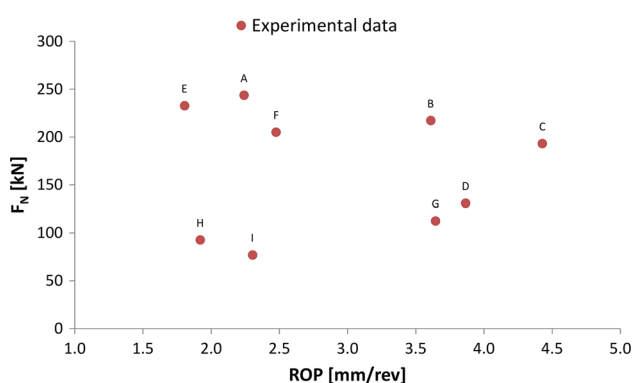
Fig. 10 Cutter normal force (F_N) versus rate of penetration (ROP)

material. Moreover, no consistent relationship between the ROP and CI was identified, as suggested by the laboratory results of Roxborough and Rispin (1973). This condition is likely due to the effect that the fracturing of the rock mass has on the ROP, as shown by several earlier studies (e.g. Gong et al. 2006; Abu Bakar et al. 2014).

The results also indicate that the size of the fragments is influenced by the rock mass characteristics; yet, a clear relationship between the parameters was not found at the examined site. In particular, it was observed that the CI does not show a consistent relationship with RMR and GSI. This condition is mainly due to the nature of
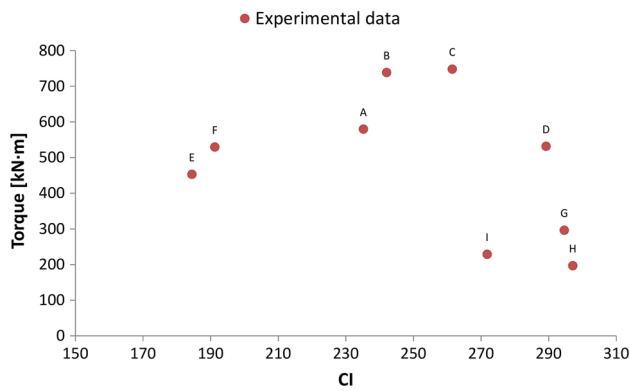
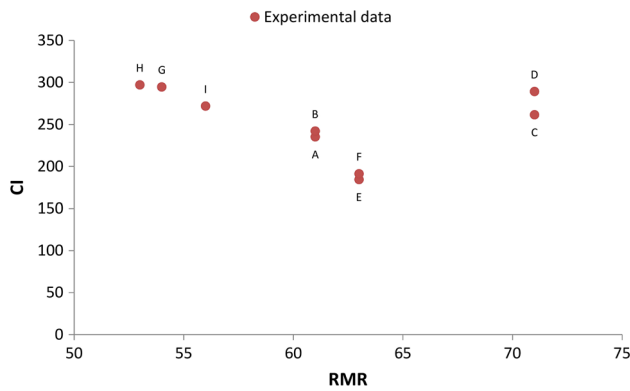**Fig. 11** Torque versus coarseness index (CI)
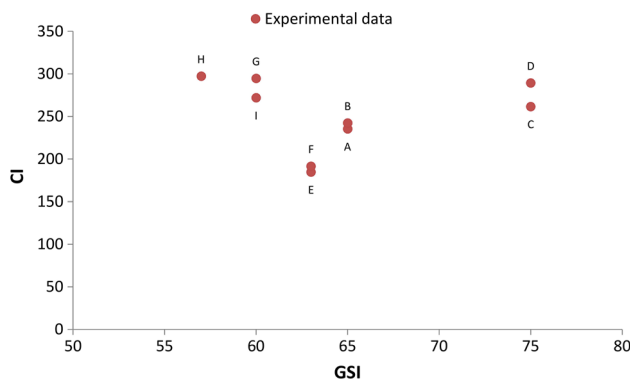

Fig. 12 Coarseness index (CI) versus RMR

Fig. 13 Coarseness index (CI) versus GSI

Fig. 14 Coarseness index (CI) versus uniaxial compression strength (UCS). Linear trendline: $CI = -2.8275 \cdot UCS + 722.53$; $R^2 = 0.676$

fracturing may involve a dual effect on the size of the debris, including a decrease in the CI due to the greater presence of fines caused by over-crushing in front of the cutterhead, as well as an increase in the CI due to the detachment of large rock fragments at the excavation face.

those geomechanical classifications, which take into account various parameters of the rock mass that influence the size of the debris with differing effects. On one hand, the influence of the characteristics of intact rock, such as the UCS, cannot be disregarded (e.g. UCS exhibited a slightly decreasing trend with respect to the CI at the study site). On the other hand, there are the conditions of the rock mass, such as the joint spacing, which did not show a significant relationship with the CI. This confirms that an increase in the rock mass
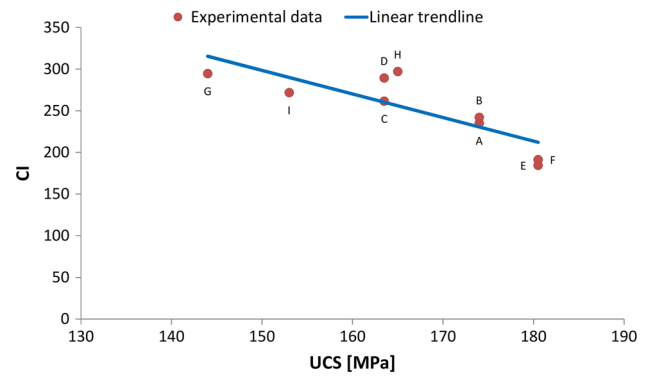
References

Abu Bakar MZ, Gertsch L, Rostami J (2014) Evaluation of fragments from disc cutting of dry and saturated sandstone. Rock Mech Rock Eng 47(5):1891–1903

Altindag R (2003) Estimation of penetration rate in percussive drilling by means of coarseness index and mean particle size. Rock Mech Rock Eng 36(4):323–332

Balci C (2009) Correlation of rock cutting tests with field performance of a TBM in a highly fractured rock formation: a case study in Kozyatagi-Kadikoy Metro Tunnel, Turkey. Tunn Undergr Space Technol 24:423–435

Bieniawski ZT (1989) Engineering rock mass classifications. Wiley, New York

Bilgin N, Copur H, Balci C (2014) Mechanical excavation in mining and civil industries. CRC Press, Boca Raton

British Standard European Norm 933-1 (2012) Tests for geometrical properties of aggregates. Determination of particle size distribution. Sieving method. BSI Standards, London

Broch E, Franklin JA (1972) The point-load strength test. Int J Rock Mech Min Sci 9:669–697

Bruland A (1998) Hard rock tunnel boring, performance data and back-mapping. Project report 1E−98. University of Science and Technology Trondheim, Trondheim

Cardu M, Rispoli A, Bilgin N (2017) Innovazioni nello scavo meccanizzato in roccia. In: MIR 2017—16° Ciclo di conferenze di Meccanica ed Ingegneria delle Rocce "Innovazione nella progettazione, realizzazione e gestione delle opere in sotterraneo". Celid, Torino, pp 55–78

Farrokh E, Rostami J (2008) Correlation of tunnel convergence with TBM operational parameters and chip size in the Ghomroud tunnel, Iran. Tunn Undergr Space Technol 23:700–710

Gertsch L, Fjeld A, Nilsen B, Gertsch R (2000) Use of TBM muck as construction material. Tunn Undergr Space Technol 15(4):379–402

Gong QM, Jiao YY, Zhao J (2006) Numerical modelling of the effects of joint spacing on rock fragmentation by TBM cutters. Tunn Undergr Space Technol 21(1):46–55

Hassanpour J, Rostami J, Zhao J (2011) A new hard rock TBM performance prediction model for project planning. Tunn Undergr Space Technol 26:595–603

Hoek E, Marinos P, Benissi M (1998) Applicability of the geological strength index (GSI) classification for weak and sheared rock masses—the case of the Athens schist formation. Bull Eng Geol Environ 57(2):151–160

International Society for Rock Mechanics (1978) Suggested methods for the quantitative description of discontinuities. In: Brown ET (ed) Rock masses. Rock characterisation testing and monitoring. Pergamon Press, Oxford, pp 320–363

Kemeny J (1994) A practical technique for determining the size distribution of blasted benches, waste dumps, and heap-leach sites. Min Eng 46(11):1281–1284

McFeat-Smith I, Fowell RJ (1977) Correlation of rock properties and the cutting performance of tunnelling machines. Proceedings of a conference on rock engineering. Newcastle University, Newcastle upon Tyne, pp 581–602

Nelson PP (1993) TBM performance analysis with reference to rock properties. In: Hudson JA (ed) Comprehensive rock engineering. Pergamon Press, Oxford, pp 261–292

Ozdemir L (1992) Mechanical excavation techniques in underground construction. Short course notebook, vol 1. Istanbul Technical University, Istanbul, pp 1–49

Parisi ME, Farinetti A, Gilli P, Brino L (2015) First results from the excavation of the Lyon—Turin Maddalena exploratory tunnel. In: ITA WTC congress and 41st general assembly; proceedings of international symposium, May 22–28, Dubrovnik, pp 0–11

Rispoli A, Ferrero AM, Cardu M, Brino L, Farinetti A (2016) Hard rock TBM performance: preliminary study based on an exploratory tunnel in the Alps. In: Ulusay R et al (eds) Rock mechanics and rock engineering: from the past to the future. Taylor & Francis Group, London, pp 469–474

Roxborough FF, Phillips HR (1975) Rock excavation by disc cutter. Int J Rock Mech Min Sci Geomech Abstr 12:361–366

Roxborough FF, Rispin A (1973) The mechanical cutting characteristics of the lower chalk. Tunn Tunn 5:45–67

Tuncdemir H, Bilgin N, Copur H, Balci C (2008) Control of rock cutting efficiency by muck size. Int J Rock Mech Min Sci 45(2):278–288